PERGAMON

International Journal of Solids and Structures 40 (2003) 2301–2320

INTERNATIONAL JOURNAL OF SOLIDS and STRUCTURES

www.elsevier.com/locate/ijsolstr

Bézier curves in the modification of boundary integral equations (BIE) for potential boundary-values problems

Eugeniusz Zieniuk *

Department of Mathematics and Physics, Institute of Computer Science, University of Bialystok, PL-15-887 Bialystok, ul. Sosnowa 64, Poland

Received 17 July 2001; received in revised form 18 December 2002

Abstract

The paper presents a modification of the classical boundary integral equation method (BIEM) for two-dimensional potential boundary values problems. The proposed modification consists in describing the boundary geometry by means of Bézier curves. As a result of this analytical modification of the BIEM, a new parametric integral equation system (PIES) was obtained. The kernels of these equations include the geometry of the boundary. This new PIES is no longer defined on the boundary, as in the case of the BIEM, but on the straight line for any given domain. The solution of the new PIES does not require a boundary discretization since it can be reduced merely to an approximation of boundary functions. To solve this PIES a pseudospectral method has been proposed and the results obtained were compared with exact solutions.

Keywords: Bézier curve; Boundary integral equation; Fourier transform; Potential problem; Parametric integral equation system

1. Introduction

Currently there exist two methods commonly used for the numerical solution of boundary problems. One is the finite element method and the other, developing dynamically in recent times, the boundary element method (BEM). In the former method the whole domain of the problem is discretized by finite elements (Zienkiewicz, 1977), whereas in the latter only the domain boundary is discretized by boundary elements (Beer and Watson, 1992; Beskos, 1987; Brebbia et al., 1984).

To increase the accuracy of the description of the boundary geometry various boundary elements were introduced. In paper (Camp and Gipson, 1991; Jonston, 1996) Overhauser elements were introduced to ensure the required continuity at the points of their joins. In papers (Jonston, 1997; Liggett and Salmon, 1981; Sen, 1995) boundary elements were described by means of spline functions, whereas in (Durodola and

* Fax: +48-85-745-7662.
E-mail address: ezieniuk@ii.uwb.edu.pl (E. Zieniuk).

0020-7683/03/$ - see front matter © 2003 Elsevier Science Ltd. All rights reserved.
doi:10.1016/S0020-7683(03)00050-7

Fenner, 1990; Gray and Soucie, 1993; Singh and Kalra, 1995) Hermite polynomials were used. Generally, boundary elements are characterized by a necessity of simultaneous approximation of the boundary geometry and boundary functions.

The necessity of simultaneous approximation mentioned above constitutes a serious problem from the point of view of the possibility of an effective boundary modification as well as application of other methods of the approximation of boundary functions.

A new system of integral equations was proposed in papers (Zieniuk, 1998; Zieniuk and Szczebiot, 1999) in which the boundary geometry approximation is separated from boundary functions. This system was obtained as a result of an analytical modification of the classical boundary integral equation method (BIEM) by Fourier transformations. The system may be applied to solve potential boundary-value problems with the domains bounded by polygons. In this system polygon segments are described by non-parametrical linear functions, whereas in paper (Zieniuk, 1999) non-linear segments are described by non-parametrical polynomials of the third degree. However, from a practical point of view, segment description by means of non-parametrical functions is still troublesome. It was necessary to set the polygon with respect to the assumed system of co-ordinates in such a way that all its segments projected as sections on one of the axis. This is due to the fact that the system of integral equations is no longer defined on the boundary as a classical BIEM but only on one of the axis of the assumed system of co-ordinates.

In paper (Zieniuk, 2001, 2002), parametric linear functions were proposed to describe the segments. Such a description is more effective because it is not directly connected with the system of co-ordinates. The parametric integral equation system (PIES) thus obtained is no longer defined on the axis of the assumed system of co-ordinates but on the straight line exclusively. The length of this line is equal to the polygon periphery. Information on the boundary line segments is contained in the PIES kernels.

In the present paper Bézier parametrical segments are proposed to describe non-linear segments of the boundary geometry. Such segments are commonly used in computer graphics (Mortenson, 1985; Faux and Pratt, 1979; Rogers and Adams, 1976) to create Bézier curves. These curves are very effective since they enable an easy modification of the boundary geometry with the help de Bézier control points and also make it possible to ensure the required continuity. Closed curves can be used to describe the boundary geometry in boundary-value problems. By introducing these curves into the classical BIEM we obtain a new PIES whose formalism takes the boundary geometry into consideration. This boundary is described by Bézier curves. The PIES thus obtained facilitates the creation and modification of the boundary geometries with the help of de Bézier control points.

In this paper the BIEM modification is exemplified by Laplace's equation as a particular case of potential problem. The proposed concept can be also applied to other potential equations. The PIES solution (unlike the classical BIEM) does not require an approximation of the boundary geometry but is reduced exclusively to the approximation of the boundary functions. The separation of the simultaneous approximation of the boundary geometry from the boundary functions in the PIES creates new possibilities of using various methods of the numerical solutions of the PIES (Zieniuk and Szczebiot, 1999). To solve this new PIES a pseudospectral method (PM) was proposed (Gottlieb and Orszag, 1977). The numerical results obtained from the testing example were compared with exact results.

2. Bézier curves used to describe boundary geometry

2.1. Cubic segment in Bézier representation

Bézier parametric cubic segment is a polynomial curve of the third degree described by four Bézier control points $\boldsymbol{V}_0$, $\boldsymbol{V}_1$, $\boldsymbol{V}_2$, $\boldsymbol{V}_3$. These points enable us to create segment shapes. A graphical presentation of such a segment is shown in Fig. 1.

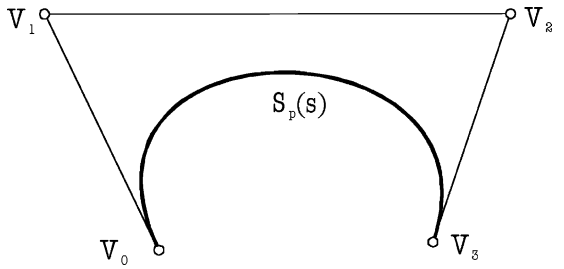

Fig. 1. Cubic segment in the Bézier representation.

The cubic segment using the Bézier control points is represented with the help of vector equation (Mortenson, 1985).

$$\boldsymbol{S}_p(s) = \boldsymbol{V}_0(1-s)^3 + \boldsymbol{V}_1 3s(1-s)^2 + \boldsymbol{V}_2 3s^2(1-s) + \boldsymbol{V}_3 s^3, \quad \boldsymbol{S}_p = [S_p^{(1)}, S_p^{2)}]^{\mathrm{T}}, \tag{1}$$

or in a simplified form

$$\boldsymbol{S}_p(s) = \sum_{j=0}^{3} \boldsymbol{V}_j \cdot B_{j,3}(s); \quad 0 \leqslant s \leqslant 1, \tag{2}$$

where the polynomials

$$B_{j,3}(s) = \frac{3!}{j!(3-j)!}(1-s)^{3-j}s^j; \quad 0 \leqslant s \leqslant 1,\ 0 \leqslant j \leqslant 3, \tag{3}$$

are Bernstein base functions of the third degree. These functions are shown in Fig. 2.

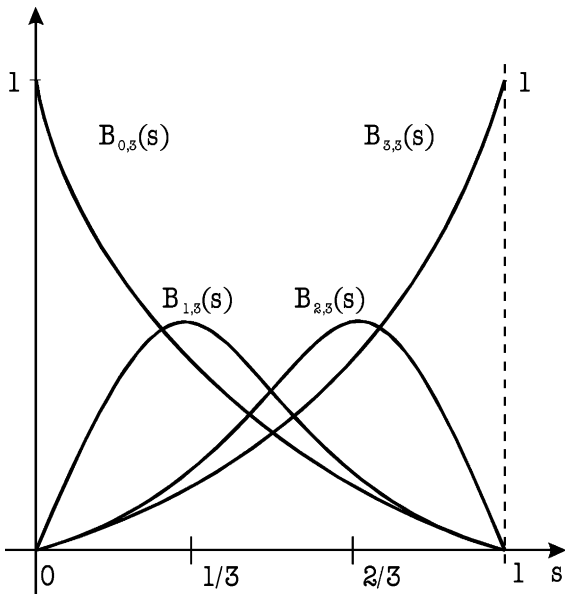

Fig. 2. Bernsten base functions of the third degree.

By differentiating the Bézier representation (1) we can present the first derivative at the segment ends using Bézier control points as:

$$\begin{aligned} \boldsymbol{S}'_p(0) &= 3(\boldsymbol{V}_1 - \boldsymbol{V}_0), \\ \boldsymbol{S}'_p(1) &= 3(\boldsymbol{V}_3 - \boldsymbol{V}_2). \end{aligned} \tag{4}$$

The cubic segment is represented with the help four Bézier control points only (1). By increasing the number of the control points we obtain polynomial segments of any degree. With the help of $n+1$ control points we can define the polynomial segment $\boldsymbol{S}_p(s)$ of pth degree. Using control points we can easily change the polynomial degree. Thus, for $n = 3$ we obtain a cubic segment, a parabolic one for $n = 2$, and for $n = 1$ the segment is reduced to the straight line.

2.2. C^1-Bézier curves composed of cubic segments

By joining Bézier segments, it is possible to define a curve described by a series of Bézier control points. A graphical presentation of such a curve is given in Fig. 3. Removing the control points brings about local changes of the curve shape.

Let control points, $\boldsymbol{V}_0$, $\boldsymbol{V}_1$, $\boldsymbol{V}_2$, $\boldsymbol{V}_3$ and $\boldsymbol{V}_0^*$, $\boldsymbol{V}_1^*$, $\boldsymbol{V}_2^*$, $\boldsymbol{V}_3^*$ denote Bézier control points for two adjacent cubic segments $\boldsymbol{S}_p(s)$ and $\boldsymbol{S}_{p+1}(s)$ which should be joined in such a way as to obtain a C^1-curve at the join point $\boldsymbol{V}_3 = \boldsymbol{V}_0^*$. It follows from the continuity requirement that condition (5) must be satisfied:

$$\boldsymbol{S}'_{p+1}(0) = \boldsymbol{S}'_p(1). \tag{5}$$

Hence, from the formulas (4) determining the first derivative we obtain the condition

$$\boldsymbol{V}_1^* - \boldsymbol{V}_0^* = \boldsymbol{V}_3 - \boldsymbol{V}_2, \tag{6}$$

i.e. the control points $\boldsymbol{V}_2 = \boldsymbol{V}_1^*$ must be symmetrical with respect to $\boldsymbol{V}_3 = \boldsymbol{V}_0^*$. A graphical interpretation of formula (6) is shown in Fig. 4.

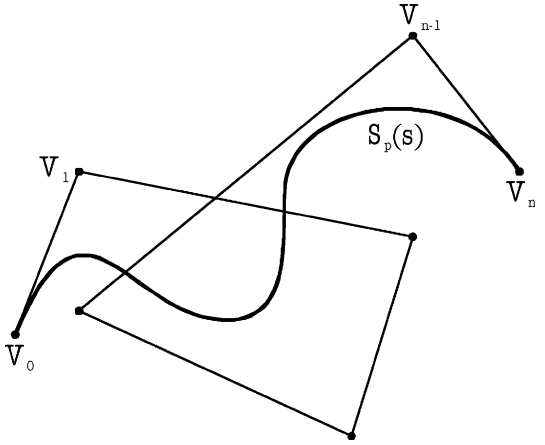

Fig. 3. Bézier curve composed of cubic segments.

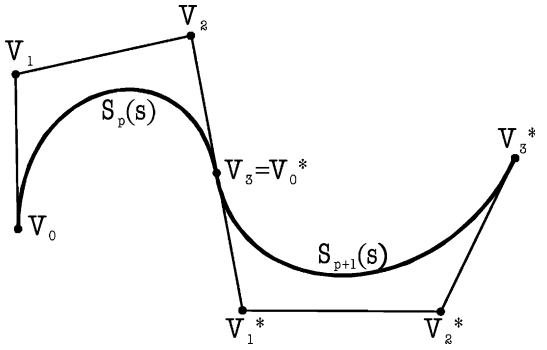

Fig. 4. Continuity condition of C^1-curve composed of Bézier segments.

2.3. C^2- Bézier curves composed of cubic segments

The curves described by C^2 equation are the curves composed of segments in such a way that the first and second derivative of the equation are continuous at the points of segment joins. Let the segments to be joined in this way be described by the control points as above.

The conditions to be satisfied can be written as follows:

1. Curve continuity condition

$$\boldsymbol{V}_0^* = \boldsymbol{V}_3. \tag{7}$$

2. Continuity condition of the first derivative at the point of segment joins

$$\boldsymbol{V}_1^* - \boldsymbol{V}_0^* = \boldsymbol{V}_3 - \boldsymbol{V}_2. \tag{8}$$

3. Continuity condition of the second derivative of the point of segment joins

$$\boldsymbol{S}''_{p+1}(0) = \boldsymbol{S}''_p(1). \tag{9}$$

Since

$$\begin{aligned} \boldsymbol{S}''_{p+1}(0) &= 6(\boldsymbol{V}_0^* - 2\boldsymbol{V}_1^* + \boldsymbol{V}_2^*), \\ \boldsymbol{S}''_p(1) &= 6(\boldsymbol{V}_1 - 2\boldsymbol{V}_2 + \boldsymbol{V}_3), \end{aligned} \tag{10}$$

and taking conditions (7) and (8) into account we obtain

$$\boldsymbol{V}_2 + (\boldsymbol{V}_2 - \boldsymbol{V}_1) = \boldsymbol{V}_1^* + (\boldsymbol{V}_1^* - \boldsymbol{V}_2^*). \tag{11}$$

Point $\boldsymbol{V}_2 + (\boldsymbol{V}_2 - \boldsymbol{V}_1) = \boldsymbol{V}_1^* + (\boldsymbol{V}_1^* - \boldsymbol{V}_2^*)$ is called de Boor's control point (Mortenson, 1985). A geometric interpretation of condition (11) is presented in Fig. 5.

By an appropriate selection of Bézier control points, we can easily join segments ensuring C^1 and C^2 continuity. Fig. 6 shows a graphical presentation of a closed curve of C^2.

The closed curve presented in Fig. 6 can be used to effectively describe the boundary geometry in BIEM. For this purpose it is necessary to modify the classical integral equations.

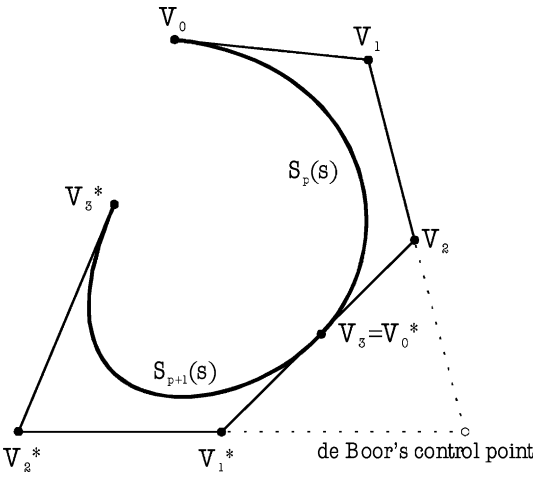

Fig. 5. Continuity condition C^2 for Bézier curve.

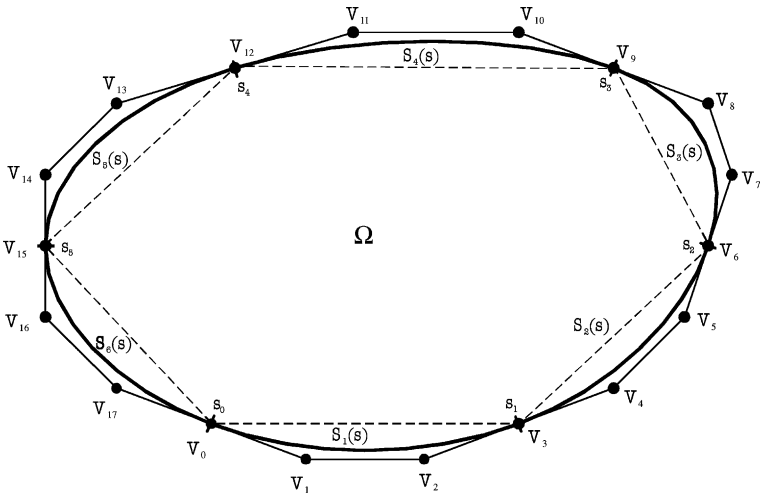

Fig. 6. Definition of boundary geometry with the Bézier curve.

3. Modification of the boundary integral equation

The boundary integral identity may be presented by means of a general formula (Green's formula) in the following form (Brebbia et al., 1984)

$$\bar{u}(\boldsymbol{x}) = \int_{\Gamma} U^*(\boldsymbol{x},\boldsymbol{y}) p(\boldsymbol{y})\,\mathrm{d}\Gamma(\boldsymbol{y}) - \int_{\Gamma} \boldsymbol{P}^*(\boldsymbol{x},\boldsymbol{y}) u(\boldsymbol{y})\,\mathrm{d}\Gamma(\boldsymbol{y}), \tag{12}$$

where

$$\bar{u}(\boldsymbol{x}) = \begin{cases} u(\boldsymbol{x}) & \text{for } \boldsymbol{x} \in \Omega \\ 0.5u(\boldsymbol{x}) & \text{for } \boldsymbol{x} \in \Gamma, \\ 0 & \text{for } \boldsymbol{x} \notin \overline{\Omega} \end{cases} \quad p(\boldsymbol{y}) \equiv \frac{\partial u(\boldsymbol{y})}{\partial n(\boldsymbol{y})} \quad \text{and} \quad \boldsymbol{P}^*(\boldsymbol{x},\boldsymbol{y}) \equiv \frac{\partial U^*(\boldsymbol{x},\boldsymbol{y})}{\partial \boldsymbol{n}(\boldsymbol{y})}.$$

If $\boldsymbol{x} \in \Gamma$ then the Green's formula (12) is the boundary integral equation (BIE). In the identity (12), an integrand $U^*(\boldsymbol{x},\boldsymbol{y})$ is the classical fundamental solution, whereas $P^*(\boldsymbol{x},\boldsymbol{y})$ is the classical singular solution.

In order to modify Green's formula the Fourier transform was applied and after its application to (12) we obtained the following transform (Zieniuk, 1998, 1999, 2001)

$$\hat{\tilde{\boldsymbol{u}}}(\boldsymbol{\xi}) = \Delta^{-1}(\boldsymbol{\xi})\{\tilde{\boldsymbol{p}}(\boldsymbol{\xi}) + \mathrm{i}[\xi_1\tilde{\boldsymbol{u}}\tilde{\boldsymbol{n}}_1(\boldsymbol{\xi}) + \xi_2\tilde{\boldsymbol{u}}\tilde{\boldsymbol{n}}_2(\boldsymbol{\xi})]\}, \tag{13}$$

where $\Delta^{-1}(\boldsymbol{\xi}) = [\xi_1^2 + \xi_2^2]^{-1}$.

In formula (13) the boundary is defined by means of the following boundary integrals:

$$\tilde{\boldsymbol{p}}(\boldsymbol{\xi}) = \int_{\Gamma} \mathrm{e}^{-\mathrm{i}(\xi_1 y_1 + \xi_2 y_2)} p(\boldsymbol{y})\,\mathrm{d}\Gamma(\boldsymbol{y}), \tag{14}$$

$$\tilde{\boldsymbol{u}}\tilde{\boldsymbol{n}}_m(\boldsymbol{\xi}) = \int_{\Gamma} \mathrm{e}^{-\mathrm{i}(\xi_1 y_1 + \xi_2 y_2)} n_m(\boldsymbol{y}) u(\boldsymbol{y})\,\mathrm{d}\Gamma(\boldsymbol{y}), \quad m = 1,2,\ \boldsymbol{y} \in \Gamma, \tag{15}$$

whereas, n_m is a directional cosine of the normal vector to the boundary Γ. The integrals (14) and (15) will be defined as boundary transforms.

We use the integral (15) to define the function transform $\tilde{\boldsymbol{u}}\tilde{\boldsymbol{n}}_m(\boldsymbol{\xi})$ on the boundary Γ. The unknown integrand $u(\boldsymbol{y})$ in (15) may be defined by means of the following Fourier formula:

$$u(\boldsymbol{y}) = \frac{1}{4\pi^2} \int_{R^2} \mathrm{e}^{\mathrm{i}(\omega_1 y_1 + \omega_2 y_2)} \hat{\boldsymbol{u}}(\boldsymbol{\omega})\,\mathrm{d}\boldsymbol{\omega}, \quad \boldsymbol{\omega} \equiv (\omega_1, \omega_2), \tag{16}$$

where the integrand $\hat{\boldsymbol{u}}(\boldsymbol{\omega})$ is given by

$$\hat{\boldsymbol{u}}(\boldsymbol{\omega}) = 2\Delta^{-1}(\boldsymbol{\omega})\{\tilde{\boldsymbol{p}}(\boldsymbol{\omega}) + \mathrm{i}[\omega_1\tilde{\boldsymbol{u}}\tilde{\boldsymbol{n}}_1(\boldsymbol{\omega}) + \omega_2\tilde{\boldsymbol{u}}\tilde{\boldsymbol{n}}_2(\boldsymbol{\omega})]\}. \tag{17}$$

The formula (17) is a particular case of the transform (13).

4. Transform of the integral equation system

After substituting (17) into (16)—and then the resulting expression into (15)—we get the convolution integral equation in the domain of Fourier transforms,

$$\tilde{\boldsymbol{u}}\tilde{\boldsymbol{n}}_m(\boldsymbol{\xi}) = \int_{R^2} \widetilde{\boldsymbol{K}}_m(\gamma_1,\gamma_2)\Delta^{-1}(\boldsymbol{\omega})\{\tilde{\boldsymbol{p}}(\boldsymbol{\omega}) + \mathrm{i}[\omega_1\tilde{\boldsymbol{u}}\tilde{\boldsymbol{n}}_1(\boldsymbol{\omega}) + \omega_2\tilde{\boldsymbol{u}}\tilde{\boldsymbol{n}}_2(\boldsymbol{\omega})]\}\,\mathrm{d}\boldsymbol{\omega}, \tag{18}$$

where the kernel is

$$\widetilde{\boldsymbol{K}}_m(\gamma_1,\gamma_2) = \frac{1}{2\pi^2} \int_{\Gamma} \mathrm{e}^{\mathrm{i}(\gamma_1 y_1 + \gamma_2 y_2)} n_m(\boldsymbol{y})\,\mathrm{d}\Gamma(\boldsymbol{y}), \quad \gamma_i = \omega_i - \xi_i. \tag{19}$$

The contour integral in (19) takes into consideration the boundary geometry of Γ. In our further considerations we divide the boundary Γ into n non-linear segments.

Therefore, after taking into consideration the segmental representation of the boundary, we may present the kernel (19) as

$$\widetilde{\boldsymbol{K}}_m(\gamma_1,\gamma_2) = \frac{1}{2\pi^2} \sum_{l=1}^{n} \int_{\Gamma_l} \mathrm{e}^{\mathrm{i}(\gamma_1 y_1 + \gamma_2 y_2)} n_m^{(l)}(\boldsymbol{y})\,\mathrm{d}\Gamma(\boldsymbol{y}), \tag{20}$$

whereas the boundary transforms $\tilde{\boldsymbol{u}}\tilde{\boldsymbol{n}}_m(\boldsymbol{\xi})$ occurring on the left hand side of (18) may be represented in the following form:

$$\tilde{\boldsymbol{u}}\tilde{\boldsymbol{n}}_m(\boldsymbol{\xi}) = \sum_{l=1}^{n} \tilde{\boldsymbol{u}}_l \tilde{\boldsymbol{n}}_m^{(l)}(\boldsymbol{\xi}). \tag{21}$$

We mark the boundary transforms $\tilde{\boldsymbol{p}}(\boldsymbol{\omega})$ and $\tilde{\boldsymbol{u}}\tilde{\boldsymbol{n}}_m(\boldsymbol{\omega})$ on individual segments on the right hand side of (18) by the index j in the following way

$$\tilde{\boldsymbol{p}}(\boldsymbol{\omega}) = \sum_{j=1}^{n} \tilde{\boldsymbol{p}}_j(\boldsymbol{\omega}), \quad \tilde{\boldsymbol{u}}\tilde{\boldsymbol{n}}_m(\boldsymbol{\omega}) = \sum_{j=1}^{n} \tilde{\boldsymbol{u}}_j \tilde{\boldsymbol{n}}_m^{(j)}(\boldsymbol{\omega}). \tag{22}$$

After substituting (21), (22) and (20) in (18) we obtain the following system of the convolution integral equations:

$$\tilde{\boldsymbol{u}}_l \tilde{\boldsymbol{n}}_m^{(l)}(\boldsymbol{\xi}) = \int_{R^2} \overline{\tilde{\boldsymbol{K}}}_m(\gamma_1, \gamma_2) \sum_{j=1}^{n} \Delta^{-1}(\boldsymbol{\omega}) \left\{ \tilde{\boldsymbol{p}}_j(\boldsymbol{\omega}) + \mathrm{i}\left[\omega_1 \tilde{\boldsymbol{u}}_j \tilde{\boldsymbol{n}}_1^{(j)}(\boldsymbol{\omega}) + \omega_2 \tilde{\boldsymbol{u}}_j \tilde{\boldsymbol{n}}_2^{(j)}(\boldsymbol{\omega}) \right] \right\} \mathrm{d}\boldsymbol{\omega}, \tag{23}$$

where

$$\overline{\tilde{\boldsymbol{K}}}_m(\gamma_1, \gamma_2) = \frac{1}{2\pi^2} \int_{\Gamma_l} \mathrm{e}^{\mathrm{i}(\gamma_1 y_1 + \gamma_2 y_2)} \boldsymbol{n}_m^{(l)}(\boldsymbol{y}) \, \mathrm{d}\Gamma(\boldsymbol{y}), \quad l = 1, 2, \ldots, n. \tag{24}$$

These boundary transforms on individual segments in (23) may be defined as follows:

$$\tilde{\boldsymbol{p}}_j(\boldsymbol{\omega}) = \int_{\Gamma_j} \mathrm{e}^{-\mathrm{i}(\omega_1 y_1 + \omega_2 y_2)} p_j(\boldsymbol{y}) \, \mathrm{d}\Gamma(\boldsymbol{y}), \tag{25}$$

$$\tilde{\boldsymbol{u}}_p \tilde{\boldsymbol{n}}_m^{(p)}(\boldsymbol{\omega}) = \int_{\Gamma_p} \mathrm{e}^{-\mathrm{i}(\omega_1 y_1 + \omega_2 y_2)} \boldsymbol{n}_m^{(p)}(\boldsymbol{y}) u_p(\boldsymbol{y}) \, \mathrm{d}\Gamma(\boldsymbol{y}), \quad \boldsymbol{\omega} = \boldsymbol{\xi}, \ p = l, j. \tag{26}$$

We shall define the segments ($\Gamma_p \equiv \boldsymbol{S}_p$) with the help of Bezier representation (1). The modelling of the segments within the boundary geometry is presented in Fig. 6.

The kernel (24) for the boundary segments in the Bézier representation is described by the following formula

$$\overline{\tilde{\boldsymbol{K}}}_m(\gamma_1, \gamma_2) = \frac{1}{2\pi^2} \int_{s_{l-1}}^{s_l} \mathrm{e}^{\mathrm{i}\left[\gamma_1 S_l^{(1)}(s) + \gamma_2 S_l^{(2)}(s)\right]} J_l(s) n_m(s) \, \mathrm{d}s, \quad s_{l-1} \leqslant s \leqslant s_l, \tag{27}$$

where

$$J_l(s) = \left[\left(\frac{\partial y_1}{\partial s} \right)^2 + \left(\frac{\partial y_2}{\partial s} \right)^2 \right]^{0.5}, \quad y_1 = \boldsymbol{S}_l^{(1)}(s), \ y_2 = \boldsymbol{S}_l^{(2)}(s).$$

The *segmental transforms* $\tilde{\boldsymbol{p}}_j(\boldsymbol{\omega})$, $\tilde{\boldsymbol{u}}_p \tilde{\boldsymbol{n}}_m^{(p)}(\boldsymbol{\omega})$ after considering Bézier segments have following form

$$\begin{aligned} \tilde{\boldsymbol{p}}_j(\boldsymbol{\omega}) &= \int_{s_{j-1}}^{s_j} \mathrm{e}^{-\mathrm{i}\left[\omega_1 S_j^{(1)}(s) + \omega_2 S_j^{(2)}(s)\right]} p_j(s) J_j(s) \, \mathrm{d}s, \\ \tilde{\boldsymbol{u}}_p \tilde{\boldsymbol{n}}_m^{(p)}(\boldsymbol{\omega}) &= \int_{s_{p-1}}^{s_p} \mathrm{e}^{-\mathrm{i}\left[\omega_1 S_p^{(1)}(s) + \omega_2 S_p^{(2)}(s)\right]} u_p(s) n_m^{(p)}(s) J_p(s) \, \mathrm{d}s, \ \ \boldsymbol{\omega} = \boldsymbol{\xi}, \ p = l, j, \end{aligned} \tag{28}$$

where

$$p_j(s) = p_j\left[S_j^{(1)}(s), S_j^{(2)}(s)\right], \quad n_m^{(p)}(s) = n_m^{(p)}\left[S_p^{(1)}(s), S_j^{(2)}(s)\right], \quad u_p(s) = u_p\left[S_p^{(1)}(s), S_p^{(2)}(s)\right].$$

The cubic segment $S_p(s)$ is given by the expression (1).

5. New parametric integral equation system

After substituting (28) and (27) into (23) we obtain the convolution integral equation in the domain of the Fourier transforms. After the application of the inverse of the Fourier transform a new PIES is obtained (Zieniuk, 1998, 1999, 2001)

$$0.5u_l(s_1) = \sum_{j=1}^{n} \int_{s_{j-1}}^{s_j} \left\{ \overline{U}^*_{lj}(s_1,s)p_j(s) - \overline{P}^*_{lj}(s_1,s)u_j(s) \right\} J_j(s)\,\mathrm{d}s, \quad s_{j-1} < s_1, s < s_j. \tag{29}$$

The kernels in the above system are functions $\overline{U}^*_{lj}(s_1,s)$ and $\overline{P}^*_{lj}(s_1,s)$ given by the following integral expression:

$$\overline{U}^*_{lj}(s_1,s) = \frac{1}{4\pi^2} \int_{R^2} \mathrm{e}^{\mathrm{i}(\omega_1\eta_1+\omega_2\eta_2)} \Delta^{-1}(\boldsymbol{\omega})\,\mathrm{d}\boldsymbol{\omega}, \tag{30}$$

$$\overline{P}^*_{lj}(s_1,s) = \frac{-i}{4\pi^2} \int_{R^2} \mathrm{e}^{\mathrm{i}(\omega_1\eta_1+\omega_2\eta_2)} \Delta^{-1}(\boldsymbol{\omega})[\omega_1 n_1^{(j)}(s) + \omega_2 n_2^{(j)}(s)]\,\mathrm{d}\boldsymbol{\omega}. \tag{31}$$

After calculation of the relatively complex integrals (30) and (31) we obtain the final expressions in the following form:

$$\overline{U}^*_{lj}(s_1,s) = \frac{1}{2\pi} \ln \frac{1}{[\eta_1^2+\eta_2^2]^{0.5}}, \tag{32}$$

$$\overline{P}^*_{lj}(s_1,s) = \frac{1}{2\pi} \frac{\eta_1 n_1^{(j)}(s) + \eta_2 n_2^{(j)}(s)}{\eta_1^2+\eta_2^2}, \tag{33}$$

where $\eta_1 = S_l^{(1)}(s_1) - S_j^{(1)}(s)$ and $\eta_2 = S_l^{(2)}(s_1) - S_j^{(2)}(s)$.

The expression (32) is a modified fundamental solution called the *boundary fundamental solution*, whereas, expression (33) is a modified singular solution called the *boundary singular solution.* These expressions constitute the modified fundamental and singular solution of the Laplace's equation. The modified solutions (32) and (33) take into account the boundary geometry in contrast to traditional solutions.

The PIES is defined for any given configuration of the boundary geometry on the straight line in a parametrical reference system. The length of the line is depend on the length of the boundary.

6. Solution in domain

Solution in domain Ω may be obtained from the transform presented by formula (13)

$$\hat{\boldsymbol{u}}(\boldsymbol{\xi}) = \Delta^{-1}(\boldsymbol{\xi})\{\tilde{\boldsymbol{p}}(\boldsymbol{\xi}) + \mathrm{i}[\xi_1 \tilde{\boldsymbol{u}}\tilde{\boldsymbol{n}}_1(\boldsymbol{\xi}) + \xi_2 \tilde{\boldsymbol{u}}\tilde{\boldsymbol{n}}_2(\boldsymbol{\xi})]\}. \tag{34}$$

In this identity, we present the boundary integrals $\tilde{\boldsymbol{p}}(\boldsymbol{\xi}), \tilde{\boldsymbol{u}}\tilde{\boldsymbol{n}}_m(\boldsymbol{\xi})$, $m = 1, 2$ by means of segmental integrals (22), in which the variable $\boldsymbol{\omega}$ is replaced by $\boldsymbol{\xi}$. In the local system of co-ordinates the integrals may be presented in the following way

$$\begin{aligned} \tilde{\boldsymbol{p}}_j(\boldsymbol{\xi}) &= \int_{s_{j-1}}^{s_j} \mathrm{e}^{-\mathrm{i}\left[\xi_1 S_j^{(1)}(s) + \xi_2 S_j^{(2)}(s)\right]} p_j(s) J_j(s)\,\mathrm{d}s, \\ \tilde{\boldsymbol{u}}_j\tilde{\boldsymbol{n}}_m^{(j)}(\boldsymbol{\xi}) &= \int_{s_{j-1}}^{s_j} \mathrm{e}^{-\mathrm{i}\left[\xi_1 S_j^{(1)}(s) + \xi_2 S_j^{(2)}(s)\right]} n_m^{(j)}(s) u_j(s) J_j(s)\,\mathrm{d}s. \end{aligned} \tag{35}$$

After substituting (35) to (34) and after the application of the inverse Fourier transform we obtain

$$u(\boldsymbol{x}) = \sum_{j=1}^{n} \int_{s_{j-1}}^{s_j} \left\{ \widehat{\overline{U}}_j^*(\boldsymbol{x}, s) p_j(s) - \widehat{\overline{P}}_j^*(\boldsymbol{x}, s) u_j(s) \right\} J_j(s)\, \mathrm{d}s, \tag{36}$$

where integrands are represented by

$$\widehat{\overline{U}}_j^*(\boldsymbol{x}, s) = \frac{1}{4\pi^2} \int_{R^2} \mathrm{e}^{\mathrm{i}(\xi_1 \overleftrightarrow{r}_1 + \xi_2 \overleftrightarrow{r}_2)} \Delta^{-1}(\boldsymbol{\xi})\, \mathrm{d}\boldsymbol{\xi}, \tag{37}$$

$$\widehat{\overline{P}}_j^*(\boldsymbol{x}, s) = \frac{-i}{4\pi^2} \int_{R^2} \mathrm{e}^{\mathrm{i}(\xi_1 \overleftrightarrow{r}_1 + \xi_2 \overleftrightarrow{r}_2)} \Delta^{-1}(\boldsymbol{\xi}) \left[\xi_1 n_1^{(j)}(s) + \xi_2 n_2^{(j)}(s) \right] \mathrm{d}\boldsymbol{\xi}. \tag{38}$$

After calculation of relatively complex integrals (37) and (38) we obtain expressions in the following explicit form

$$\widehat{\overline{U}}_j^*(\boldsymbol{x}, s) = \frac{1}{2\pi} \ln \frac{1}{[\overleftrightarrow{r}_1^2 + \overleftrightarrow{r}_2^2]^{0.5}}, \tag{39}$$

$$\widehat{\overline{P}}_j{}^*(\boldsymbol{x}, s) = \frac{1}{2\pi} \frac{\overleftrightarrow{r}_1 n_1^{(j)}(s) + \overleftrightarrow{r}_2 n_2^{(j)}(s)}{\overleftrightarrow{r}_1^2 + \overleftrightarrow{r}_2^2}, \tag{40}$$

where $\overleftrightarrow{r}_1 = x_1 - S_j^{(1)}(s)$ and $\overleftrightarrow{r}_2 = x_2 - S_j^{(2)}(s)$.

The former expression (39) is a modification of the fundamental Laplace's solution and can be called a *fundamental solution in the domain*. The latter expression (40) can be called a *singular solution in the domain*. These modifications take into account the boundary geometry defined by means of Bézier curves.

7. Numerical solution

The PSIE solution does not require the discretization of the boundary and it reduces exclusively to the approximation of boundary functions $u_j(s)$, $p_j(s)$ on individual segments. For the solution (29)—the PM (Zieniuk and Szczebiot, 1999; Gottlieb and Orszag, 1977) is applied. The boundary functions are approximated by means of the following expressions

$$p_j(s) = \sum_{k=0}^{N} p_j^{(k)} T_j^{(k)}(s), \quad u_j(s) = \sum_{k=0}^{N} u_j^{(k)} T_j^{(k)}(s), \tag{41}$$

where $u_j^{(k)}$, $p_j^{(k)}$ are unknown coefficients, N—is a number of coefficients on segment, and $T_j^k(s)$ are the global base functions on individual segments—Chebyshev polynomials.

Inserting (41) into (29) we obtain the equation which reduces to a system of algebraic equations in respect to the unknown coefficients.

$$0.5 u_l(s_1) = \sum_{j=k}^{n} \sum_{k=0}^{N} \left\{ p_j^{(k)} \int_{s_{j-1}}^{s_j} \overline{U}_{lj}^*(s_1, s) - u_j^{(k)} \int_{s_{j-1}}^{s_j} \overline{P}_{lj}^*(s_1, s) \right\} T_j^{(k)}(s) J_j(s)\, \mathrm{d}s. \tag{42}$$

Eq. (42), having been represented at collocation points ($n \times N$) reduces to a system of algebraic equations with respect to the unknown coefficients $p_j^{(k)}$ or $u_j^{(k)}$. On solving the system of algebraic equations and having made use of approximating expressions (41) we obtain the unknown functions on boundary Γ_p. Having found the functions on the boundary we can obtain the solution in domain Ω on the basis of the integral identity (36).

8. Practical application of the method

Five different testing examples illustrating the accuracy and effectiveness of the proposed method compared with other well-known analytical and numerical methods are presented. When comparing the results special attention was paid to:

- number of input data necessary to define the problem for each of the numerical methods used,
- accuracy of the obtained results in comparison with exact solutions,
- number of algebraic equation system required.

The first testing example is concerned with temperature distribution in a cylinder of infinite length. The main purpose of the example is to show the effectiveness of defining boundary geometry by Bézier control points in contrast to BEM. The accuracy of the obtained results is compared with the results obtained by BEM and the analytical method.

The second testing example illustrates a possibility of defining boundary geometry by curvilinear segments and also by Bézier segments of the first degree. In this example temperature distribution in a living room defined by a small number of corner points is analyzed. The obtained results are compared with solutions obtained by well-known methods (Hartmann, 1989).

The next two examples deal with an analysis of twisted bars of various cross-sections. In the third example, a triangular cross-section defined by first degree segments is considered. The fourth example gives an analysis of an elliptical cross-section whose boundary geometry is defined by third degree Bézier curves. The obtained results are compared with other well-known numerical and analytical methods.

The fifth testing example illustrates some possibilities of defining various types of boundary geometries. In this example boundary geometry is defined by first and third degree segments.

8.1. Example 1: Temperature distribution in the cylinder

Temperature distribution in a cylinder of infinite length and radius R is shown in Fig. 7. We need to find steady temperature field in the cylinder. The problem can be described by

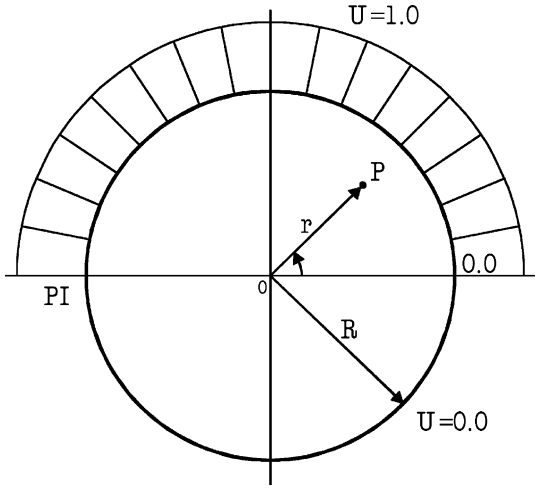

Fig. 7. Cylinder geometry of infinite length with a given temperature on its surface.

$$\frac{\partial^2 u}{\partial r^2}+\frac{1}{r}\frac{\partial u}{\partial r}+\frac{1}{r^2}\frac{\partial^2 u}{\partial \theta^2}=0, \tag{43}$$

i.e. by the Laplace's equation (Brebbia et al., 1984) in a polar coordinate system with the following boundary conditions

$$u(R,\theta)=\begin{cases} u=1.0, & 0\leqslant\theta\leqslant\pi \\ u=0.0, & \pi<\theta<2\pi \end{cases}. \tag{44}$$

The analytical solution is

$$u(R,\theta)=\frac{1}{2}+2\sum_{n=1}^{\infty}\frac{1}{\pi n}\left(\frac{r}{R}\right)^n\sin n\theta, \quad n=1,3,5, \tag{45}$$

A practical way of defining boundary geometries by third degree Bézier curves is shown in Fig. 8. To give a relatively exact description of the boundary only four segments of the third degree S_1, S_2, S_3, S_4 are required and to define the segments we need 12 Bézier control points (see Fig. 8). Four of them, V_0, V_3, V_6, V_9, that lie on the boundary are interpolating points, whereas the remaining eight points (not lying on the boundary) are approximating points. However, to define boundary geometry by Bézier curves all of these points must be given.

For a practical definition of boundary geometry only 4 points $V_0=P_0$, $V_3=P_1$, $V_6=P_2$, $V_9=P_3$ lying on the boundary are given, whereas the remaining missing control points are determined numerically after solving a system of algebraic equations. This system is obtained under the condition that the segments at their join points, P_0, P_1, P_2, P_3, keep continuity class C^2.

The solution on the boundary for boundary problem (43) can be obtained using PIES represented by (29) and the solution in domain Ω by (36). The obtained results for $U=R=1$ at points 1–8 inside the cylinder (see Fig. 8) are compared with the results in (Brebbia et al., 1984) obtained by the use of constant elements. The results are shown in Table 1.

As seen in Table 1, to obtain near-analytical solutions, in the case of BEM, it is necessary to use as many as 48 constant elements. It means that we need to give as many as 48 nodes on the boundary and also solve

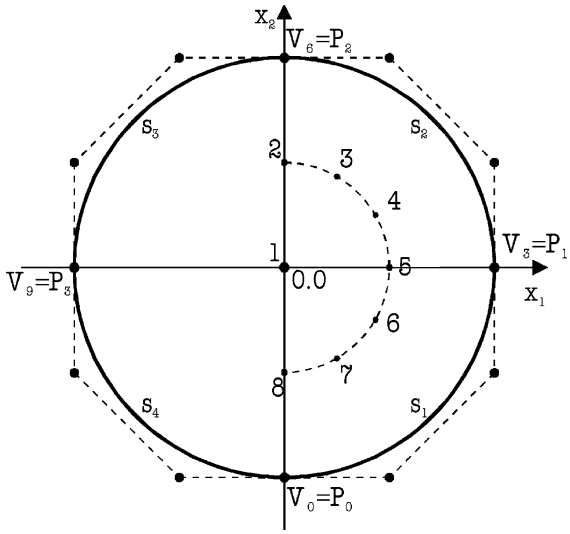

Fig. 8. Definition of the cross-section of the boundary geometry by Bézier control points.

Table 1
Temperature at points inside the cylinder

Points	BEM (Brebbia et al., 1984)		Analytical solutions	PIES, $N = 2$
	24 elements	48 elements		
1	2	3	4	5
1	0.500	0.500	0.500	0.50000
2	0.799	0.796	0.795	0.79535
3	0.776	0.774	0.773	0.77301
4	0.689	0.688	0.687	0.68751
5	0.500	0.500	0.500	0.50000
6	0.311	0.312	0.313	0.31248
7	0.224	0.226	0.227	0.22691
8	0.201	0.204	0.205	0.20464

48 algebraic equations. It must be also noted that the condition of continuity C^2 at the join points of the boundary elements is not satisfied.

Using PIES and formula (36) high accuracy (see Table 1) was obtained by defining the boundary using merely four points (P_0, P_1, P_2, P_3) and solving a system of only eight algebraic equations. A smaller number of input data required for the definition of the problem as well as a smaller system of algebraic equations to be solved, considerably shortens the computation time as compared to BEM. If we take high accuracy of the obtained results in this example and compare them with the exact solution, it can be stated that the proposed method is very effective.

8.2. Example 2: Temperature distribution in L-shaped living room

It is very effective to define boundary geometry by Bézier curves as they can be easily described by polynomials of any given degree. Increasing or decreasing polynomial degrees practically reduces to either addition or subtraction of Bézier points. Due to the above it is possible to use PIES to solve boundary problems with boundaries modelled by curves described by either high or low degree polynomials.

In this example, Bézier segments of the first degree are used to solve a polygon domain problem that is reduced to determining temperature distribution in an L-shaped living room (see Fig. 9). The walls of the

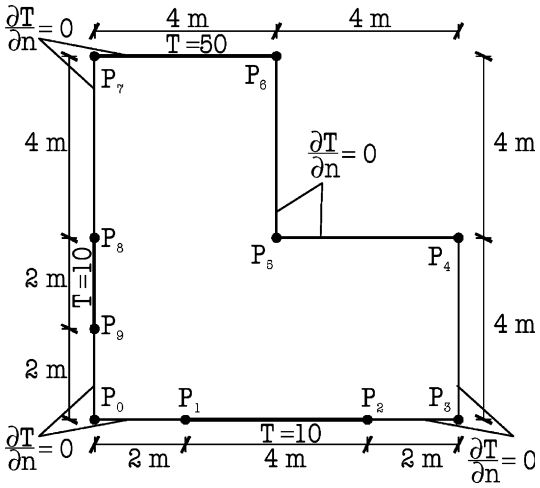

Fig. 9. Temperature distribution in an L-shape domain. Domain defined by points.

living room are considered to be perfectly isolated so that the flux at the walls is zero, i.e., $\partial T/\partial n = 0$. The temperature of the window panes is assumed to 10 °C and the temperature of the chimney at the upper end of the living room is assumed to be 50 °C. The temperature distribution T in the living room is the function that satisfies boundary conditions and the Laplace equation, i.e.,

$$\frac{\partial^2 T}{\partial x_1^2} + \frac{\partial^2 T}{\partial x_2^2} = 0 \quad \text{in } \Omega. \tag{46}$$

Fig. 9 presents the defining of the living room geometry by first degree Bézier curves. The task is practically reduced to giving a small number of Bézier control points. These points, for linear segments, are the living room corner points, P_0, P_3, P_4, P_5, P_6, P_7. Due to the fact that there are different boundary conditions imposed along some of the walls, it is necessary to introduce additional points P_1, P_2, P_8, P_9 (see Fig. 9), at which changes of the types of boundary conditions take place. To give an exact definition of the room domain as well as the boundary conditions only 10 points are required. Hence the boundary was divided into $n = 10$ line segments.

This example was solved by quadrature element method (Zhong and He, 1998) and BEM (Hartmann, 1989) and also by PIES using different numbers of expressions N of the approximating series (41). Fig. 10 gives the results obtained at various living room points using different methods.

8.3. Example 3: Torsion of a bar of a triangular cross-section

In this testing example PIES was used for analysing the stress field at various points of a twisted bar of triangular cross-section (Fig. 11). Such a cross-section can be easily defined by first degree Bézier points using only three corner points, P_0, P_1, P_2. To solve the same problem by BEM we need to give many more nodes.

The problem prismatic bar torsion can be solved by resolving the Laplace's equation using the following boundary conditions

$$u(\boldsymbol{x}) = \frac{x_1^2 + x_2^2}{2}. \tag{47}$$

An exact solution for function $u(\boldsymbol{x})$ resulting from the resolution of the Laplace's equation and shear stresses in the considered cross-section, is represented by formulas (Hromadka and Lai, 1987)

$$u(\boldsymbol{x}) = (x_1^3 - 3x_1x_2^2)/2a + 2a^2/27, \tag{48}$$

$$\tau_{x_1x_3} = -\mu\theta(x_2 + 3x_1x_2/a), \tag{49}$$

$$\tau_{x_2x_3} = \mu\theta\left[\left(3x_2^2 - 3x_1^2\right)/2a + x_1\right]. \tag{50}$$

Table 2 presents exact results for function $u(\boldsymbol{x})$ calculated from formulas (48) and approximated results $\hat{\boldsymbol{u}}(\boldsymbol{x})$ obtained by a well-known numerical method—CBEM (Hromadka and Lai, 1987), and also by the method proposed here, making use of PIES. Table 2 also includes relative errors $|\varepsilon_u| = |(u - \hat{\boldsymbol{u}})/u|$ for numerical methods.

It is evident that the proposed method enables us to calculate function $\hat{\boldsymbol{u}}(\boldsymbol{x})$ with much greater accuracy than CBEM.

The stress field was calculated using the same methods and the results obtained at particular points of the triangular cross-section are shown in Table 3. Shear stresses calculated by a well-known numerical method CBEM and the proposed method (based on PIES) were compared with exact solutions ((49) and (50)). The comparison is presented in the form of a relative error shown in columns 5 and 10 for CBEM and columns 7 and 12 for PIES. As can be seen, stresses $\widehat{\tau}_{x_1x_3}$, $\widehat{\tau}_{x_2x_3}$ were also calculated with high accuracy.

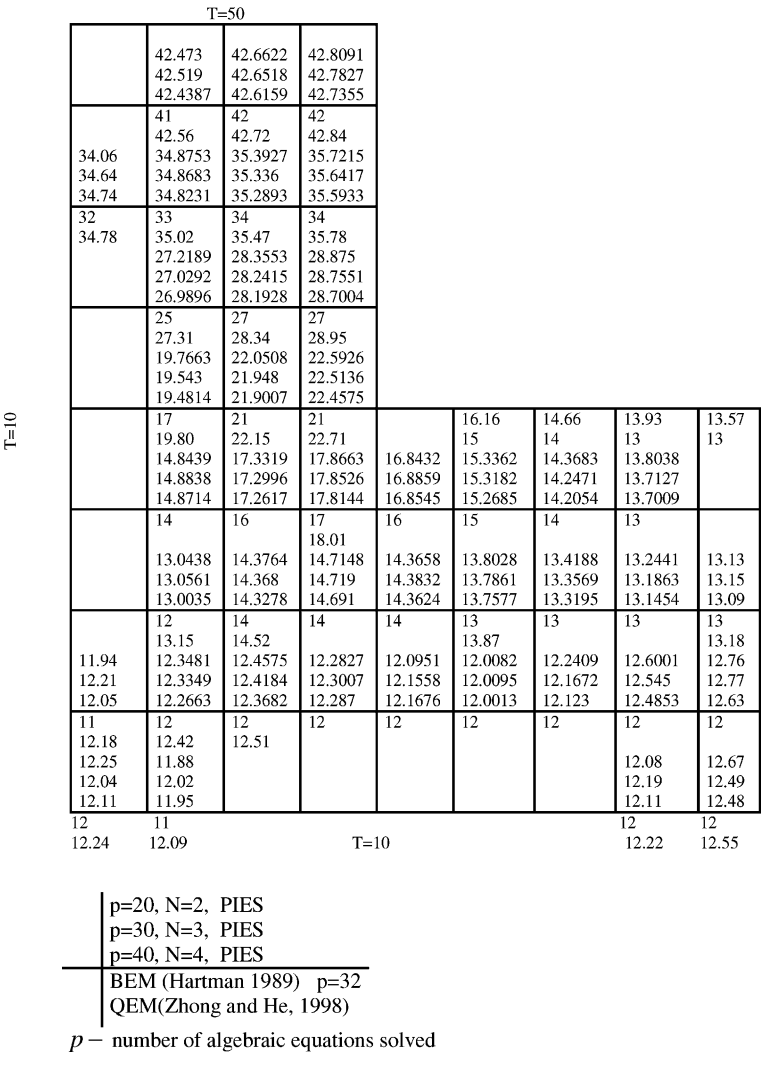

Fig. 10. Results for temperature distribution problem.

8.4. Example 4: Torsion of a bar of elliptical cross-section

In this example, PIES is used for analysing stress states in a twisted bar of elliptical cross-section described by

$$\frac{x_1^2}{a^2}+\frac{x_2^2}{b^2}=1. \tag{51}$$

To give a practical definition of such a cross-section for PIES we apply Bézier curvilinear segments of the third degree joined together and keeping continuity C^2. Graphical representation of this cross-section and the way of its definition is shown in Fig. 12. To define the geometry of the cross-section, it was necessary to define merely four interpolating Bézier points P_0, P_2, P_4, P_6. To obtain a very exact definition, it was enough

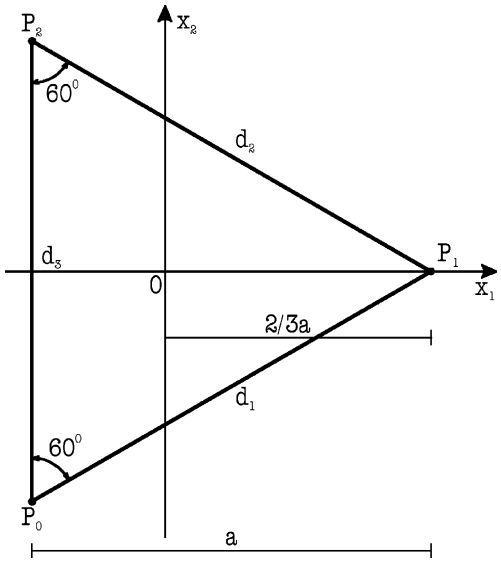

Fig. 11. Definition of cross-section by corner points.

Table 2
Comparison of exact and approximated solutions

x_1	x_2	u-analyt	$\hat{u}$-CBEM	$\lvert\varepsilon_u\rvert$ (%) CBEM	$\hat{u}$-PIES	$\lvert\varepsilon_u\rvert$ (%) PIES
1	2	3	4	5	6	7
−0.50	0.0	0.64583	0.6557	1.53	0.64585	0.00310
−0.0	0.0	0.66667	0.6763	1.44	0.66668	0.00150
0.5	0.0	0.68750	0.6969	1.37	0.68751	0.00145
1.0	0.0	0.83333	0.8417	1.01	0.83336	0.00360
1.5	0.0	1.22917	1.2302	0.08	1.22809	0.08786
−0.50	0.50	0.70833	0.7180	1.36	0.70833	0.00000
0.0	0.50	0.66666	0.6763	1.44	0.66668	0.00300
0.5	0.50	0.62500	0.6347	1.55	0.62443	0.09120
−0.50	1.0	0.89583	0.9046	0.98	0.89594	0.01228

to give additional four points P_1, P_3, P_5, P_7. Thus, to get a very exact boundary definition, a total eight interpolating points were required. In comparison with BEM, this number is considerably smaller.

The problem is solved by the Laplace's equation with boundary conditions (47). The analytical solutions for functions $u(\boldsymbol{x})$ resulting from the resolution of the Laplace's equation and shear stresses in the considered domain, take the following form (Hromadka and Lai, 1987)

$$u(\boldsymbol{x}) = (x_1^2 + x_2^2)/2 - a^2b^2\left\{\frac{x_1^2}{a^2} + \frac{x_2^2}{b^2} - 1\right\}\Big/(a^2 + b^2),$$

$$\tau_{x_1x_3} = -\mu\theta 2x_2a^2/(a^2 + b^2), \tag{52}$$

$$\tau_{x_2x_3} = \mu\theta 2x_1b^2/(a^2 + b^2).$$

Table 4 presents exact solutions for function $u(\boldsymbol{x})$ and approximated results $\hat{\boldsymbol{u}}(\boldsymbol{x})$. The table also gives shear stresses $\widehat{\tau}_{x_1x_3}$, $\widehat{\tau}_{x_2x_3}$ at different points of the cross-section obtained by PIES for $a = 2$, $b = 1$.

Table 3
Comparison of exact and approximated solutions

x_1	x_2	$\tau_{x_1x_3}$ analytic	$\widehat{\tau}_{x_1x_3}$ CBEM	$\lvert\varepsilon_{\tau_{x_1x_3}}\rvert$ (%) CBEM	$\widehat{\tau}_{x_1x_3}$ PIES	$\lvert\varepsilon_{\tau_{x_1x_3}}\rvert$ (%) PIES	$\tau_{x_2x_3}$ analytic	$\widehat{\tau}_{x_2x_3}$ CBIE	$\lvert\varepsilon_{\tau_{x_2x_3}}\rvert$ (%) CBIE	$\widehat{\tau}_{x_2x_3}$ PIES	$\lvert\varepsilon_{\tau_{x_2x_3}}\rvert$ (%) PIES
1	2	3	4	5	6	7	8	9	10	11	12
−0.5	0.0	0.0	0	–	4.223e−16	–	−0.625	−0.63	0.80	−0.62468	0.0512
−0.0	0.0	0.0	0	–	1.761e−16	–	0.0000	0.0	0.0	0.0	0.0
0.5	0.0	0.0	0	–	3.936e−16	–	0.3750	0.37	1.33	0.37500	0.0000
1.0	0.0	0.0	0	–	1.197e−15	–	0.5000	0.50	0	0.49951	0.0980
1.5	0.0	0.0	−0.01	–	−1.41e−15	–	0.3750	0.37	1.33	0.35274	5.9360
−0.5	0.5	−0.25	−0.25	0.0	−0.24971	0.1160	−0.500	−0.49	2.00	−0.50024	0.0480
0.0	0.5	−0.50	−0.50	0.0	−0.49991	0.0180	0.1250	0.12	4.00	0.12503	0.0240
0.5	0.5	−0.75	−0.75	0.0	−0.76496	1.9947	0.5000	0.50	0	0.49834	0.3320
−0.5	1.0	−0.50	−0.50	0.0	−0.49961	0.0780	−0.125	−0.13	4.0	−0.12761	2.0880

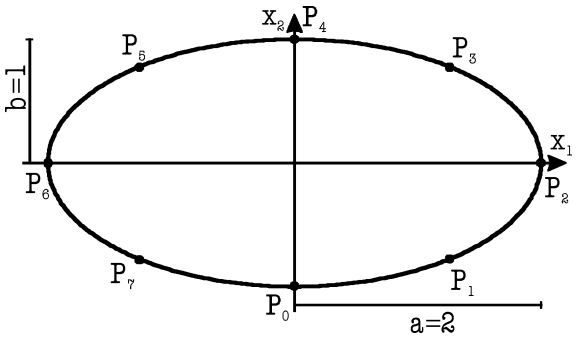

Fig. 12. Boundary definition by Bézier control points.

The results presented in Table 4 show that the approximation of both function $\hat{u}(\boldsymbol{x})$ and shear stresses $\widehat{\tau}_{x_1x_3}$, $\widehat{\tau}_{x_2x_3}$ was obtained with great accuracy.

8.5. Example 5: Complex boundary geometry

In the fifth example we present some possibilities of defining various boundary geometry by Bézier curves using polynomials of different degrees. In this example, boundary geometry is described by segments of the first and third degree.

The example considers a problem of two-dimensional steady fluid flow (in the x_1-direction) between parallel walls with a cylinder as an obstacle, as shown in Fig. 13. By using centreline symmetry and mid-stream antisymmetry, only a quarter of domain marked *abcde* need be analysed (Durodola and Fenner, 1990). Boundary conditions are imposed in terms of a stream function u.

To ensure a very accurate definition of this domain, it is necessary to give merely six boundary points P_i, $i = 0, 1, \ldots, 5$. The results of the proposed method are shown in Table 5. They have been compared with the known examples obtained by BEM for various boundary elements. In paper Durodola and Fenner (1990) to solve Example 5 Hermitian cubic elements (HCE) are used for various numbers of posed nodes, whereas in Alarcon et al. (1979) Lagrange quadratic elements are applied.

Table 4
Comparison of exact and approximated solutions

x_1	x_2	u analytic	$\hat{u}$-PURC	$\lvert\varepsilon_u\rvert$ (%)	$\tau_{x_1x_3}$ analytic	$\hat{\tau}_{x_1x_3}$ PURC	$\lvert\varepsilon_{\tau_{x_1x_3}}\rvert$ (%)	$\tau_{x_2x_3}$ analytic	$\hat{\tau}_{x_2x_3}$ PURC	$\lvert\varepsilon_{\tau_{x_2x_3}}\rvert$ (%)
1	2	3	4	5	6	7	8	9	10	11
0.0	0.0	0.80000	0.80039	0.04850	0.0	−6.00e−08	–	0.000	1.291e−08	–
0.5	0.0	0.87500	0.87528	0.03154	0.0	2.079e−07	–	0.200	0.20060	0.29950
1.0	0.0	1.10000	1.09954	0.04182	0.0	4.175e−07	–	0.400	0.40258	0.64475
1.5	0.0	1.47500	1.47285	0.14576	0.0	−4.35e−06	–	0.600	0.60311	0.51817
0.0	0.25	0.78125	0.78165	0.05171	−0.400	−0.39989	0.02650	0.000	−1.10e−07	–
0.25	0.25	0.80000	0.80040	0.04975	−0.400	−0.39977	0.05700	0.100	0.10007	0.06800
0.75	0.25	0.95000	0.95016	0.01726	−0.400	−0.39896	0.26075	0.300	0.30118	0.39500
1.25	0.25	1.25000	1.24885	0.09200	−0.400	−0.39902	0.24375	0.500	0.50429	0.85800
1.75	0.25	1.70000	1.69650	0.20588	−0.400	−0.40883	2.20850	0.700	0.70244	0.34886
0.0	0.50	0.72500	0.72542	0.05807	−0.800	−0.80004	0.00462	0.000	−1.83e−07	–
0.25	0.50	0.74375	0.74421	0.06225	−0.800	−0.79978	0.02800	0.100	0.09969	0.30810
0.75	0.50	0.89375	0.89431	0.06299	−0.800	−0.79784	0.26963	0.300	0.30034	0.11300
1.25	0.50	1.19375	1.19315	0.05026	−0.800	−0.79613	0.48375	0.500	0.50536	1.07240
0.0	0.75	0.63125	0.63160	0.05418	−1.200	−1.20071	0.05917	0.000	1.691e−08	–
0.25	0.75	0.65000	0.65047	0.07200	−1.200	−1.20031	0.02583	0.100	0.09903	0.97190
0.50	0.75	0.70625	0.70705	0.11285	−1.200	−1.19950	0.04167	0.200	0.19858	0.70850
0.75	0.75	0.80000	0.80114	0.14188	−1.200	−1.20100	0.08333	0.300	0.30248	0.82500

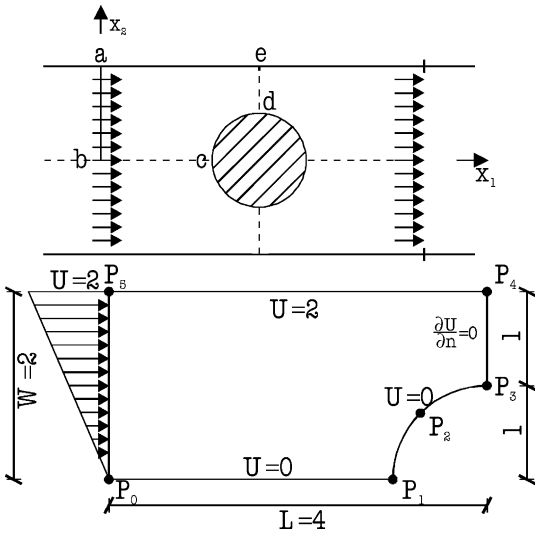

Fig. 13. Flow around a cylinder in an infinite field and the model with boundary conditions.

On the basis of the examples presented in Section 8, it can be noted that the proposed method, in contrast to well-known numerical methods, proved more effective because it requires a smaller number of input date and it is reduced to solving a smaller number of algebraic equations.

The effectiveness of the proposed method was tested on the examples taken from the literature quoted. They allowed us to compare only the accuracy of calculations and the number of the input data required to define the problem. However, the results given in the literature did not allow us to compare the compu-

Table 5
Comparison of approximated solutions

x_1	x_2	HCE[a]				LBEM[b] (32)	(PIES) (6)
		(25)	(27)	(33)	(39)		
1	2	3	4	5	6	7	8
4.00	1.00	0.0000	0.0000	0.0000	0.0000	0.0000	0.0000
4.00	1.16	0.3852	0.3854	0.3863	0.3868	0.3898	0.3852
4.00	1.33	0.7523	0.7528	0.7517	0.7516	0.7548	0.7523
4.00	1.54	1.1631	1.1637	1.1642	1.1640	1.1666	1.1631
4.00	1.76	1.5695	1.5698	1.5703	1.5701	1.5712	1.5695
4.00	2.00	2.0000	2.0000	2.0000	2.0000	2.0000	2.0000

In columns 3–7 values in round brackets give the number of node points and in column 8 the number of boundary points.
[a] Durodola and Fenner (1990).
[b] Alarcon et al. (1979).

tation time for each of the methods. Considering high effectiveness of the proposed method, further research is being conducted to solve more complex problems including the computation time in comparison with the traditional numerical methods.

9. Conclusion

In the paper an original PIES for solving of the boundary-value problems is presented with a special application to effective numerical solutions.

The main results of the research work are as follows:

- Modification of classical BIE so as to arrive at the PIES, for which numerical solutions do not require discretization of boundary and which reduce to approximation of boundary functions only.
- For the approximation of these boundary functions PM was proposed, which was shown to be very effective and gave, contrary to BEM, continuous solutions on individual segments of boundary.
- Such solutions make it possible to perform calculation, of unknown values at any chosen points on the boundary without the necessity of solving algebraic equation systems again.
- In the new method to obtain a comparable accuracy as in BEM a smaller system of algebraic equations has to be solved.
- Modification of the boundary geometry can be performed with the help of a small number of Bézier control points.
- In the PIES an approximation of the boundary functions is not directly connected with boundary geometry therefore its free modification does not have a direct influence on the algorithm of the boundary function approximation.

References

Alarcon, E., Martin, A., Paris, F., 1979. Boundary elements in potential and elasticity theory. Comput. Struct. 10, 351–362.

Beer, G., Watson, J.O., 1992. Introduction to finite and boundary element methods for engineers. John Wiley & Sons, Chichester and New York.

Beskos, D.E., 1987. Boundary element methods in mechanics. North-Holand, Amsterdam.

Brebbia, C.A., Telles, J.C.F., Wrobel, L.C., 1984. Boundary element techniques, theory and applications in engineering. Springer-Verlag, New York.

Camp, C.V., Gipson, G.S., 1991. Overhauser elements in boundary element analysis. Math. Comput. Model. 15 (3–5), 59–69.
Durodola, J.F., Fenner, R.T., 1990. Hermitian cubic boundary elements for two-dimensional potential problems. Int. J. Numer. Meth. Engng. 30, 1051–1062.
Faux, I., Pratt, M.J., 1979. Computational Geometry for Design and Manufacture. John Wiley & Sons, New York.
Gottlieb, D., Orszag, S.A., 1977. Numerical Analysis of Spectral Methods. SIAM, Philadelphia.
Gray, L.J., Soucie, C.S., 1993. A Hermite interpolation algorithm for hypersingular boundary integrals. Int. J. Numer. Meth. Engng. 36, 2357–2367.
Hartmann, F., 1989. Introduction to Boundary Elements—Theory and Applications. Springer-Verlag, Berlin.
Hromadka II, T.V., Lai, C., 1987. The Complex Variable Boundary Element Method in Engineering Analysis. Springer-Verlag, New York.
Jonston, P.R., 1996. Second order Overhauser elements for boundary element analysis. Math. Comput. Model. 26, 61–74.
Jonston, P.R., 1997. C^2-continuous elements for boundary element analysis. Int. J. Numer. Meth. Engng. 40, 2087–2108.
Liggett, J.A., Salmon, J.R., 1981. Cubic spline boundary elements. Int. J. Numer. Meth. Engng. 17, 543–556.
Mortenson, M., 1985. Geometric Modelling. John and Sons, Chichester.
Rogers, D.F., Adams, J.A., 1976. Mathematical Elements for Computer Graphics. McGraw-Hill, New York.
Sen, D., 1995. A cubic-spline boundary integral method for two-dimensional free-surface flow problems. Int. J. Numer. Meth. Engng. 38, 1809–1830.
Singh, K.M., Kalra, M.S., 1995. Application of cubic Hermitian algorithms to boundary element analysis of heat conduction. Int. J. Numer. Meth. Engng. 38, 2639–2651.
Zhong, H., He, Y., 1998. Solution of Poisson and Laplace equations by quadrilateral quadrature element. Int. J. Solids Struct. 35, 2805–2819.
Zieniuk, E.,1998. Analytical modification of the boundary integral equations for the boundaries approximated by linear segments. Bull. Soc. Sciences et Lettres de Łódź, serie: Recherches sur les Dé formmations, vol. XXVI, pp. 71–82.
Zieniuk, E., Szczebiot, R.,1999. Modification of the boundary geometry in boundary value problems based on the new system of integral equations. In: Proc. 5 Workshop PTSK Simulation in Research and Development, Warsaw, pp. 355–366.
Zieniuk, E., 1999. New integral equation systems for boundary value-problems with cubic polinomial deformation of the boundary. Bulletin de la Societe des Sciences et des Lettres deŁódź, serie: Recherches sur les Déformmations, vol. XXVIII, pp. 103–113.
Zieniuk, E., 2001. Potential problems with polygonal boundaries by a BEM with parametric linear functions. Engng. Anal. Boundary Elem. 25/3, 185–190.
Zieniuk, E., 2002. A new integral identity for potential polygonal domain problems described by parametric linear functions. Engng. Anal. Boundary Elem. 26/10, 897–904.
Zienkiewicz, O., 1977. The Finite Element Methods. McGraw-Hill, London.